DALTON TRANSACTIONS

ACCEPTED MANUSCRIPT

Boron induced structure modifications in Pd-Cu-B system: new Ti_2Ni-type derivative borides Pd_3Cu_3B and $Pd_5Cu_5B_2$[#]

Oksana Sologub[1,*], Leonid P. Salamakha[1], Gaku Eguchi[1], Berthold Stöger[2], Peter F. Rogl[3], Ernst Bauer[1]

[1]Institute of Solid State Physics, TU Wien, A-1040 Vienna, Austria

[2]Institute for Chemical Technologies and Analytics, TU Wien, A-1040 Vienna, Austria

[3]Institute of Materials Chemistry and Research, University of Vienna, A-1090 Vienna, Austria

Abstract

The formation of two distinct derivative structures of Ti_2Ni-type, interstitial Pd_3Cu_3B and substitutive $Pd_5Cu_5B_2$, has been elucidated in Pd-Cu-B alloys from analysis of X-ray single crystal and powder diffraction data and supported by SEM. The metal atom arrangement in the new boride Pd_3Cu_3B (space group $Fd\bar{3}m$, W_3Fe_3C-type structure, a=1.1136(3) nm) follows the pattern of atom distribution in the CdNi-type structure. $Pd_5Cu_5B_2$ (space group $F\bar{4}3m$, a=1.05273(5) nm) exhibits a non-centrosymmetric substitutive derivative of the Ti_2Ni-type structure. The reduction of symmetry on passing from Ti_2Ni-type structure to $Pd_5Cu_5B_2$ corresponds to the loss of the $\bar{3}$ axis delivered by an ordered occupation of the Ni position (32*e*) by dissimilar atoms, Cu and B. In both structures, the boron atom has only contact to Pd forming $[BPd_6]$ octahedra in Pd_3Cu_3B and $[BPd_6]$ trigonal prisms in $Pd_5Cu_5B_2$. Neither a perceptible homogeneity range nor mutual solid solubility was observed for two compounds at 600 °C, while in as cast conditions $Pd_5Cu_5B_2$ exhibits extended homogeneity range formed by a partial substitution of Cu atoms (in 24*f*) by Pd ($Pd_{5+x}Cu_{5-x}B_2$, $0 \le x \le 1$). Electrical resistivity measurements performed on Pd_3Cu_3B as well as on Pd-poor and Pd-rich termini of $Pd_{5+x}Cu_{5-x}B_2$

annealed at 600 °C and in as cast conditions respectively demonstrated the absence of any phase transitions for this compounds in the temperature region from 0.3 K to 300 K.

* Corresponding author *E-mail address: oksana.sologub@univie.ac.at.*

#Electronic supplementary information (ESI) available. CCDC 1444769-1444771. For ESI and crystallographic data in CIF or other electronic format see DOI ...

Introduction

The Ti_2Ni structure[1] exhibits a face-centered cubic unit cell (space group $Fd\bar{3}m$, no. 227) with 96 atoms (Ti1 in 48*f* (*x*,⅛,⅛), *x*=0.436; Ti2 in 16*c* (0,0,0); Ni1 in 32*e* (*x*,*x*,*x*), *x*=0.213; Z=32) and dimension a=1.1278(1) nm. The Ti1 atoms (48*f* site) form a network of [Ti_6] vertex-sharing octahedra centered at the vacant 16*d* (½,½,½) site. Ni1 atoms (32*e* site) occur in tetrahedral groups (centered at empty 8*a* (⅛,⅛,⅛)) with each face of every tetrahedron being capped by a Ti2 atom on a 16*c* site, thus forming a super-tetrahedron. Each super-tetrahedron is connected to four super-tetrahedra of inverse orientation to build an infinite framework interpenetrating with the network of octahedra. Complementary, the structure can be described as arrangement of four face-connected irregular icosahedra ([$Ti2Ni1_6Ti1_6$], Ti2 in 16*c*) located in four diametrally organized octants of the unit cell.

The most distinguished feature of the Ti_2Ni-type structure is a rich variety of interstitial sites available for small atoms of the elements like H, C, N, O. Since Westgren's first determination of the so called η-carbide structure W_3Fe_3C (filled up derivative of Ti_2Ni with C in [W_6] octahedral voids (16*d*, ½,½,½)),[2] innumerable examples of phases containing two or more transition metals and carbon,[3-11] nitrogen[12-15] or oxygen[16-21] have been observed including fully ordered quaternary examples such as Ti_3NiAl_2N and others[22]. More recently, the complex Ti_2Ni-type metal nitrides and hydrides attract a considerable attention as promising catalytic[23,24] and hydrogen storage[25,26] materials, respectively. In many of these systems the "pure" Ti_2Ni-type compound does not exist but interstitial atoms are required to stabilize the η-carbide structure.[27] Population of different voids of the parent structure results in different stoichiometry of Ti_2Ni-type derivative compounds according to neutron powder and X-ray single crystal diffraction data of e.g. A_3M_3X (for X=C, N, O in 16*d*, A and M stays for transition metal in 48*f* and 16*c* sites respectively), Ti_2NiH (H in 16*d*, 8*b* and 8*a*), Mo_6Co_6C (C in 8*b*) as well as the recently reported new boride structure Mg_8Rh_4B[28] (B in 8*a*). Deviation from A_2M stoichoimetry is observed also for several pure binary compounds of the CdNi-type (Cd in 48*f* and Ni in 16*c* and 32*e* atom sites).[29-31]

Besides the stabilized A_2MX_x phases formed by inclusion of an X-element atom into the vacant sites of the metal atom framework, the Ti_2Ni-type structure has a large number of

substitutive representatives among binary, ternary and multinary systems due to its ability to accommodate a variety of combinations of metals on the metal atom sites.[32]

A completely ordered ternary Ti_2Ni-type derivative structure has been encountered from X-ray powder diffraction for the series of silicides, A_3SiNi_2 (A=V, Mn, Zn, Nb, Ta) and Nb_3SiCo_2, as well as for Zn_3GeNi_2 (structure type Mn_3Ni_2Si, space group $Fd\bar{3}m$, Si (or Ge) in 16*c* (Ti2) site),[33] and confirmed by single crystal X-ray diffraction for Mg_3AlPt_2.[34] Among boride systems, the only Re_3Al_2B phase was suggested to be isostructural with Mn_3Ni_2Si[35] from X-ray powder diffraction data. In addition to the Mn_3Ni_2Si-type structure, an ordered distribution of atoms has also been reported for a series of rare earth rich phases, RE_4TX, crystallizing with the lower symmetric space group $F\bar{4}3m$ in which two RE atoms, T and X, occupy the split atom sites of Ti1 and Ni1 of the parent Ti_2Ni (T=Co, Ni, Ru, Rh, Pd, Ir, Pt; X=Mg, In, Cd).[36,37]

Despite the Cu-Pd(Pt)-B systems are parts of the multinary alloy system Ti-Ni-Pd-Pt-Cu used as high temperature shape-memory alloys,[38,39] nothing is known about the effect of boron addition on formation and crystal structure of compounds in Cu-Pd(Pt)-B systems.

Recently we reported on the synthesis, crystal structure and electrical conductivity of a new boride $(Pt_{1-x}Cu_x)_3Cu_2B$ (x=0.33) which adopts a B-filled β-Mn-type structure and exhibits a superconducting transition at about 2 K.[40] In our current study we examined the formation, crystal structure, transport properties and electronic state of ternary phases in a comparable concentration range of the Pd-Cu-B system.

Experimental

Synthesis and phase analysis

Alloys were prepared from ingots of thoroughly re-melted pieces of palladium foil or sponge (Ögussa, Austria, 99.99 mass%), Cu shot (2-6mm, 99.999 mass%, ChemPur, Germany) and crystalline boron (ChemPur, Germany, 99.4 mass%) by repeated arc melting under argon. The arc-melted buttons were wrapped in tantalum foil and vacuum-sealed in a quartz tube for annealing at 600 °C for 240 hours. The alloys obtained yielded high crystallinity and brittleness. Lattice parameters and standard deviations were determined by least square refinements of room temperature X-ray powder diffraction (XRD) data obtained from a Guinier-Huber image plate employing monochromatic $CuK_{\alpha 1}$ radiation (or alternatively $FeK_{\alpha 1}$ radiation) and Ge as internal

standard (a_{Ge}=0.565791 nm). Qualitative analysis has been performed from the results of Rietveld refinements of X-ray powder diffraction data (program FULLPROF[41]). For precise quantitative analysis of the Pd/Cu ratio, the annealed samples were polished using standard procedure and were examined by scanning electron microscopy (SEM) using a Philips XL30 ESEM with EDAX XL-30 EDX-detector.

Electrical resistivity

Electrical resistivity of the compounds described above was studied using an a.c. bridge (Lakeshore) in the range from room temperature down to 0.3 K.

Electronic band structure calculation

Electronic band structure of ordered $Pd_5Cu_5B_2$ and Pd_3Cu_3B were calculated using the WIEN2k package [42] employing the full potential linearized augmented plane wave (FLAPW) method with generalized-gradient approximation (GGA) exchange correlation potential. Structural parameters obtained from this study were used for the calculations, and the muffin-tin radii were taken as 2.28 a.u. (Pd), 2.31 a.u. (Cu), and 1.69 a.u. (B) for $Pd_5Cu_5B_2$, and 2.27 a.u. (Pd), 2.24 a.u. (Cu), and 1.68 a.u. (B) for Pd_3Cu_3B. The cutoff energy of the LAPW basis was settled at 6.0 Ry.

Single crystal X-ray diffraction studies

Prismatically shaped single crystals suitable for X-ray diffraction studies were isolated from fragmented alloys. The crystals were measured on a four-circle Bruker APEX II diffractometer equipped with a CCD detector (κ-geometry, Mo Kα radiation); orientation matrices and unit cell parameters were derived using the APEX II software.[43] Multi-scan absorption correction was applied using the program SADABS; frame data were reduced to intensity values applying the SAINT-Plus package.[44] The structures were solved by direct methods and refined with the SHELXS-97 and SHELXL-97 programs,[45,46] respectively. Further details concerning the experiments are summarized in Table 1.

Results and discussion

Structure determination for $Pd_5Cu_5B_2$ and $Pd_{5+x}Cu_{5-x}B_2$

X-ray single crystal diffraction data indexing procedure for the crystal selected from the alloy $Pd_{42}Cu_{41}B_{17}$ annealed at 600 °C led to a cubic F-centered unit cell with lattice constants a=1.05273(5) nm. The observed extinctions were compatible with the space groups $Fm\bar{3}m$,

$F\bar{4}3m$, $F432$, $F23$ and $Fm\bar{3}$ (WinGX program package[47]) of which the noncentrosymmetric $F\bar{4}3m$ was confirmed to be correct by subsequent successful structure solution and refinement against F^2. Structure solution applying direct methods resulted in four metal atom positions, two of which (24*g* and 16*e*) were assigned to Pd and the remaining two (24*f* and 16*e)* to Cu. Boron was found on a 16*e* site from the analysis of the electron densities peaks in difference Fourier maps. Refinement converged quickly to reliability factors as low as R_{F2}=0.0138 and wR_{F2}=0.0265 applying anisotropic displacement parameters for the metal atoms and isotropic displacement parameters for boron. A refinement with free occupation factors yielded full occupancies of all atom sites leading to the formula $Pd_5Cu_5B_2$.

An X-ray powder diffraction spectrum recorded from the as-cast sample $Pd_{50}Cu_{33}B_{17}$ and unit cell dimensions of single crystal selected from the same alloy suggested isotypism with the $Pd_5Cu_5B_2$ structure. Analogously, direct methods applied to the single crystal data in the space group $F\bar{4}3m$ delivered a structure solution with two sites of Pd and two sites of Cu, one of which, namely 24*f* (*x*,0,0), *x*=0.18223(8) showed a considerably larger electron density. Refinement of occupancy parameters assuming mixed population for this atom site resulted in 68.2% Cu+31.8% Pd. The boron atom position was readily found in the difference Fourier map. A refinement of occupancy parameters for the remaining metal atoms sites showed full occupancies by only one type of atom leading to the formula $Pd_{5.95}Cu_{4.05}B_2$ in good agreement with EPMA data on Pd:Cu ratio equal 1.5. The calculations converged to final reliability factors R_{F2}=0.0198 and wR_{F2}=0.0244.

The crystals were not twinned by inversion (Flack parameters 0.00(4) and 0.00(7) for $Pd_5Cu_5B_2$ and $Pd_{5+x}Cu_{5-x}B_2$ respectively). The relevant crystallographic data for the two compounds are given in Table 1; for bond lengths values see Table 2.

Table 1 X-ray single crystal structure data[a]

Parameter/Compound	Pd_3Cu_3B	$Pd_5Cu_5B_2$	$Pd_{5+x}Cu_{5-x}B_2$ (x=0.95)
Nominal composition	$Pd_{42.85}Cu_{42.85}B_{14.30}$	$Pd_{41.7}Cu_{41.7}B_{16.6}$	$Pd_{49.6}Cu_{33.8}B_{16.6}$
Space group	$Fd\bar{3}m$; No. 227, origin at inversion center	$F\bar{4}3m$; No. 216	
Structure type	W_3Fe_3C	$Pd_5Cu_5B_2$	
Formula from refinement	Pd_3Cu_3B	$Pd_5Cu_5B_2$	$Pd_{5.95}Cu_{4.05}B_2$
Range for data collection	$5.18°<\theta<32.47°$	$3.35°<\theta<32.33°$	$3.33°<\theta<35.04°$
Crystal size	$45x45x25\mu m^3$	$45x45x35\mu m^3$	$40x40x40\mu m^3$
a [nm]	1.1136(3)	1.05273(5)	1.05981(5)
Reflections in refinement	124 $F_o>4\sigma(F_o)$ of 142 (meas. 3096)	244 $F_o>4\sigma(F_o)$ of 246 (meas. 256)	270 $F_o>4\sigma(F_o)$ of 281 (meas. 299)
Mosaicity	<0.45	<0.45	<0.45
Number of variables	14	21	21
$R_F^2=\Sigma\lvert F_0^2-F_c^2\rvert/\Sigma F_0^2$	0.0104	0.0138	0.0198
Flack parameter	-	0.00(4)	0.00(7)
GOF	1.059	1.222	1.144
Extinction (Zachariasen)	0.00010(2)	0.00011(2)	0.00012(1)
M1;	**48*f*** $(x,⅛,⅛)^b$; x=0.42918(2);	**24*g*** $(x,¼,¼)^b$; x=0.55796(5);	**24*g*** $(x,¼,¼)^b$; x=0.55784(5);
occ.;	1.00 Pd1;	1.00 Pd1;	1.00 Pd1;
U_{11}[c], $U_{22}=U_{33}$, U_{23}[e]	0.096(2), 0.075(1), -0.005(1)	0.067(2), 0.087(2), -0.027(2)	0.074(2), 0.110(2), -0.030(2)
M2;		**24*f*** (x,0,0); x=0.17730(8);	**24*f*** (x,0,0); x=0.18223(8);
occ.;		1.00 Cu1;	0.682(3)Cu1+0.318(3)Pd11;
U_{11}, $U_{22}=U_{33}$, U_{23}[e]		0.097(4), 0.083(3), -0.041(3)	0.151(4), 0.108(3), -0.049(3)
M3;	**32*e*** (x,x,x); x=20870(3);	**16*e*** (x,x,x); x=0.16673(6);	**16*e*** (x,x,x); x=0.16755(6);
occ.;	1.00 Cu1;	1.00 Cu2;	1.00 Cu2;
$U_{11}=U_{22}=U_{33}$, $U_{23}=U_{13}=U_{12}$	0.096(2), 0.003(1)	0.060(2), -0.002(2)	0.081(2), 0.000(2)
B1;	**16*d*** (½,½,½);	**16*e*** (x,x,x); x=0.6119(5);	**16*e*** (x,x,x); x=0.6130(6);
occ.; U_{iso}[d]	1.00 B1; 0.14(1)	1.00 B1; 0.12(2)	1.00 B1; 0.15(2)
M4;	**16*c*** (0,0,0);	**16*e*** (x,x,x); x=0.40473(4);	**16*e*** (x,x,x); x=0.40491(4);
occ.;	1.00 Cu2;	1.00 Pd2;	1.00 Pd2;
$U_{11}=U_{22}=U_{33}$, $U_{23}=U_{13}=U_{12}$	0.102(2), -0.007(2)	0.059(1), -0.006(1)	0.078(1), -0.009(1)
Residual density; max; min [el/nm^3]x10^3	0.48; -0.57	0.92; -0.92	1.78; -1.21

[a] crystal structure data are standardized using the program Structure Tidy[48], [b] origin at 0,0,0, [c,d] anisotropic (U_{ij}) and isotropic (U_{iso}) atomic displacement parameters are given in [10 nm^2], [e] $U_{13}=U_{12}=0$

Structure determination for Pd_3Cu_3B

Single crystal X-ray intensities for the crystal which was selected from the alloy $Pd_{43}Cu_{43}B_{14}$ annealed at 600 °C were indexed with an F-centered cubic unit cell with a lattice parameter a=1.1136(3) nm. Systematic absences in the diffraction data were consistent with two space groups, $Fd\bar{3}m$ and $Fd\bar{3}$, of which the centrosymmetric one proved to be correct during structure solution and refinement. Three metal atom positions have been assigned and refined in a straightforward manner; the boron site was easily located in the difference Fourier map. Refinement of occupancy and displacement parameters proceeded successfully to small values of reliability factors (R_{F2}=0.0104 and wR_{F2}=0.0141, max/min residual electron density 0.48/-0.57

e/nm^3 x10^3) revealing a completely ordered distribution of atoms (Table 1). Selected interatomic distances are listed in Table 2.

The structural parameters obtained from Rietveld powder data refinements for $Pd_{42}Cu_{41}B_{17}$, $Pd_{50}Cu_{33}B_{17}$ and $Pd_{43}Cu_{42}B_{15}$ samples are consistent with those refined from the single crystals (Supporting information Fig. S1a-c).

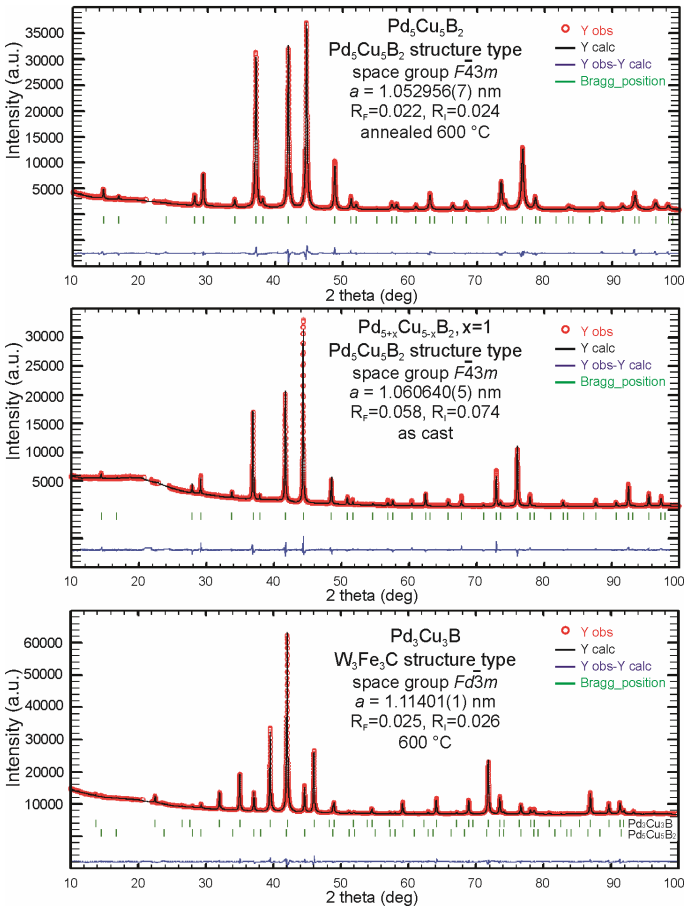

Fig. S1 Powder X-ray data, including Rietveld fit and residuals, for $Pd_5Cu_5B_2$, $Pd_{5+x}Cu_{5-x}B_2$ (x=1) and Pd_3Cu_3B. For the latter structure, Rietveld refinement has been carried out for the XPD data of the $Pd_{43}Cu_{42}B_{15}$ alloy.

Table 2 Selected interatomic distances (in 10 nm)

Pd_3Cu_3B				
Pd1–2 B1 2.1207(6)	Cu1-3 Cu2 2.4134(6)	Cu2–6 Cu1 2.4134(6)	B1 - 6 Pd1 2.1207(6)	
- 2 Cu1 2.6394(8)	- 3 Cu1 2.637(1)	-6 Pd1 2.8030(8)		
- 2 Cu1 2.7867(8)	- 3 Pd1 2.6394(8)			
- 2 Cu2 2.8030(8)	- 3 Pd1 2.7867(8)			
- 4 Pd1 2.9118(8)				
- 4 Pd1 3.0839(9)				
$Pd_5Cu_5B_2$				
Pd1–2 B1 2.133(5)	Cu1-2 Cu2 2.4847(6)	Pd2–3 B1 2.195(5)	Cu2-3 Cu2 2.4715(9)	B1–3 Pd1 2.133(5)
-2 Cu2 2.6706(8)	-4 Cu1 2.6396(9)	-3 Cu2 2.7220(7)	-3 Cu1 2.4847(6)	-3 Pd2 2.195(5)
-4 Cu1 2.8079(3)	-2 Pd2 2.7828(8)	-3 Cu1 2.7828(8)	-3 Pd1 2.6706(8)	
-2 Pd2 2.8122(5)	-4 Pd1 2.8079(3)	-3 Pd1 2.8122(5)	-3 Pd2 2.7220(7)	
-4 Pd1 2.8591(5)		-3 Pd2 2.8367(5)		
$Pd_{5+x}Cu_{5-x}B_2$, x=0.95				
Pd1–2 B1 2.135(6)	M2-2 Cu2 2.5161(6)	Pd2–3 B1 2.222(6)	Cu2-3 Cu2 2.4715(9)	B1–3 Pd1 2.135(6)
-2 Cu2 2.6894(8)	-4 M2 2.7313(9)	-3 Cu2 2.7400(8)	-3 M2 2.5161(6)	-3 Pd2 2.222(6)
-4 M2[a] 2.8128(3)	-2 Pd2 2.7569(9)	-3 M2 2.7569(9)	-3 Pd1 2.6894(8)	
-2 Pd2 2.8315(5)	-4 Pd1 2.8128(3)	-3 Pd1 2.8315(5)	-3 Pd2 2.7400(8)	
-4 Pd1 2.8801(5)		-3 Pd2 2.8504(6)		

[a] M2=0.682(3)Cu1+0.318(3)Pd11

Description of the $Pd_5Cu_5B_2$ and $Pd_{5+x}Cu_{5-x}B_2$ crystal structures

The nearest atom environment of Pd1 has the shape of a tetrahedron formed by two B and two Cu atoms; ten additional atoms are located at longer distances from Pd1 building a 14-vertices polyhedron (Fig. 1b). Pd2 has 15 neighbouring atoms (Fig. 1c). Cu2 is located inside an icosahedron formed by 12 metal atoms (Fig. 1e). Similarly, Cu1 (or M2=(0.682(3)Cu1+0.318(3)Pd11 in $Pd_{5+x}Cu_{5-x}B_2$) is coordinated by twelve metal atoms which form a polar bi-capped heptagonal prism (Fig. 1d). The boron atom is trigonal-prismatically coordinated by six palladium atoms (Fig. 1h).

The geometry of the $Pd_5Cu_5B_2$ (as well as $Pd_{5+x}Cu_{5-x}B_2$) structure can be conveniently described using the nested polyhedra approach adopted by Chabot et al (1981).[49] The structure exhibits the assembly of two types of nested units which are located in opposite octants of the unit cell (Fig. 1a). The geometric unit composed of two tetrahedra (small inner and large outer formed by Cu2 and Pd2 respectively) around the vacant site 4*c* (¼,¼,¼) and enveloped by an inner octahedron and outer cubo-octahedron (formed by Pd1 and Cu1(or M2) respectively) was first recognized in γ-brass phases (26 atoms, Fig. 1g).[50-52] The set of nested polyhedra in the opposite octant is produced of an empty palladium octahedron (centered in 4*d* (¾,¾,¾), four faces of which are capped by tetrahedrally oriented boron atoms. Along with the outer shell,

geometrically composed of a cubo-octahedron formed by Cu1 (or M2), the nested unit involving boron amounts 22 atoms and corresponds to the one, which was found for the first time in the Ti_2Ni structure.[1] Four faces of palladium octahedra of the Ti_2Ni-subunit serve as the bases of boron filled trigonal prisms [$BPd1_3Pd2_3$]. Accordingly, four of such groups belonging to different octants of the $Pd_5Cu_5B_2$ unit cell interlink via common Pd2-Pd2 edges of trigonal prisms to form empty [$Pd2_4$] tetrahedra around the Wyckoff site 4*b* (½,½,½). An enlarged view of the trigonal prisms linkage in the $Pd_5Cu_5B_2$ structure is given in Fig. 1h.

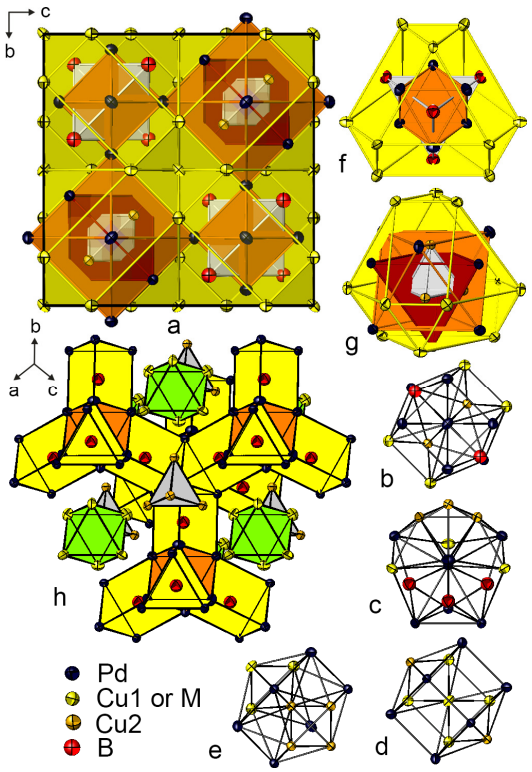

Fig. 1 $Pd_5Cu_5B_2$ structure as an arrangement of linked nested γ-brass and Ti_2Ni units (slab within $0.44 \leq x \leq 1.06$). Atoms are interlinked only for better visualization of different shells (a). Coordination polyhedra of atoms: Pd1 (b), Pd2 (c), Cu1(M1) (d) and Cu2 (e). The enlarged view of Ti_2Ni (f) and γ-brass (g) units. A framework of [BPd_6] trigonal prisms interlinked via empty [Pd_6] octahedra (centered in (4d (¾,¾,¾), orange) and empty [Pd_4] tetrahedra (centered in 4*b* (½,½,½), not visible) embedding empty [$Cu1_6$] octahedra (centered in 4*a* (0,0,0), green) and empty [$Cu2_4$] tetrahedra (centered in 4*c* (½,½,½), grey) (h).

According to the γ-brass cluster model,[53-55] the $Pd_5Cu_5B_2$ structure is built of four γ-brass type nested units which are located in opposite octants of the unit cell and condense via common Cu1(M2) vertices around an empty octahedron centered at 4*a* (0,0,0) as well as via Pd-Pd bonds. The remaining octants are filled with four tetrahedrally oriented B atoms; the boron atoms are not interconnected but bonded to the Pd atoms of the octahedral shell of the γ-brass clusters.

Description of the Pd_3Cu_3B structure

Coordination polyhedron of Pd1 is a bi-capped heptagonal prism with 4 additional atoms (Fig. 2b). Cu1 and Cu2 are located inside icosahedra formed by 12 metal atoms (Figs. 2c and 2d). The boron atom is octahedrally coordinated by six palladium atoms (Fig. 2e). The corner-shared $[BPd1_6]$ octahedra form a three-dimensional pyrochlore framework exhibiting large cages around the Wyckoff sites 32*e* and 16*c* occupied by Cu atoms.

Alike $Pd_5Cu_5B_2$, the Pd_3Cu_3B structure is geometrically composed of two kinds of building blocks located in opposite octants of the unit cell (Fig. 2a). However while the γ-brass substructure in Pd_3Cu_3B reminds that of $Pd_5Cu_5B_2$ featuring the same order of nested polyhedra but exhibiting the replacement of atom species in the atomic aggregates (inner and outer tetrahedra are formed by copper atoms only, but octahedra and cubo-octahedra are exclusively composed of palladium atoms), the nested polyhedra in the units located in the opposite octants are organized in a different way with respect to $Pd_5Cu_5B_2$. Due to inclusion of B into Wyckoff site 16*d* (½,½,½), the inner assembly of atoms geometrically relate to distorted *stella octangula* composed of two tetrahedra formed by copper and boron atoms, which interpenetrate the palladium octahedron such a way that the triangular pyramids are added to each of its faces. Despite the somewhat different geometry of the core of the boron-hosting nested polyhedra, the total number of atoms along with the outer shell (palladium cubo-octahedron) corresponds to that observed in γ-brass block (26 atoms). In the framework of the γ-brass cluster model description,[53-55] the two tetrahedrally oriented groups of atoms, viz. four Cu and four B serve as the spacers in the assembly of four γ-brass nested units in the Pd_3Cu_3B structure.

Structure relationships

Pd_3Cu_3B is the inclusion variant of the Ti_2Ni structure, where B occupies the 16*d* site. No report exists in the literature on the formation of ternary borides with this type of atom arrangement,

however, the parent W_3Fe_3C-type compound and related carbides (the so-called η6-carbide and η12-carbide phases) have been extensively studied due to their importance in steel production. Similarly to the W_3Fe_3C structure exhibiting a CW_6- and Fe- substructures, one observes in Pd_3Cu_3B a kind of segregation of atoms into a Cu- sublattice formed by vertex interlinked super-tetrahedra of inverse orientation and a network of $[BPd1_6]$ vertex-sharing octahedra clustered around the octahedral 8*b* (⅜,⅜,⅜) site (Figs. 3a and 3b), for which no evidence of the existence of additional interstitial atoms has been found from single crystal X-ray data. No residual electron density has been encountered in the 8*a* (⅛,⅛,⅛) site (at 0.164 nm and 0.245 nm from tetrahedrally orientated Cu1 and Cu2 respectively) as well, in contrast to Mg_8Rh_4B[28] where boron was found at the center of two nested Mg_4Rh_4 tetrahedra.

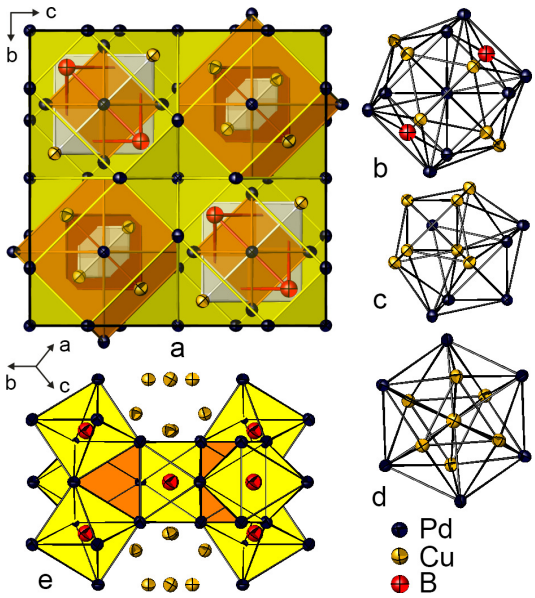

Fig. 2 Pd_3Cu_3B unit cell as arrangement of linked nested polyhedra (for better comparison with $Pd_5Cu_5B_2$ structure, the unit cell is displaced from the origin by ⅛,⅛,⅛). Coordination polyhedra of atoms: Pd1 (b), Cu1 (c) and Cu2 (d). Four boron filled octahedra (yellow colour) sharing faces with empty octahedra (orange) (e).

$Pd_5Cu_5B_2$ represents a new type of a noncentrosymmetric Ti_2Ni derivative boride structure with an ordered metal atom distribution. Ti1 (48*f*), Ti2 (16*c*) and Ni1 (32*e*) (space group $Fd\bar{3}m$) are replaced by Cu1 (24*f*) and Pd1 (24*g*), Pd2 (16*e*), Cu2 (16*e*) and B1 (16*e*),

respectively (space group $F\bar{4}3m$). Similarly to the pair $MgCu_2$—$AuBe_5$, the symmetry reduction in the $Pd_5Cu_5B_2$ structure corresponds to the loss of the $\bar{3}$ axis ($F\bar{4}3m$ is the *translationengleiche* subgroup of index 2 of $Fd\bar{3}m$) and occurs due to the ordered occupation of the Ni1 atom position by atoms with significantly different atomic radii, viz. Cu and B. The results on ternary $Pd_5Cu_5B_2$ can be compared to the findings for the RE-M-X systems (RE - rare earth metal, M - transition metal, X - Mg, Cd, In) which exhibit a large family of RE_4MX structures[36,37] (space group $F\bar{4}3m$) where the symmetry reduction is caused by the ordered distribution of Rh and X atoms on the Ni1 atom position in the Ti_2Ni structure, while Ti1 and Ti2 atom sites are populated by only one kind of atoms, namely RE. In contrast to RE_4MX, the Ti positions of the parent Ti_2Ni structure are occupied by Pd1, Cu1 and Pd2 in an ordered manner in the $Pd_5Cu_5B_2$ structure; as elucidated from X-ray single crystal and powder diffraction, the Cu1 site is prone to Pd/Cu substitution.

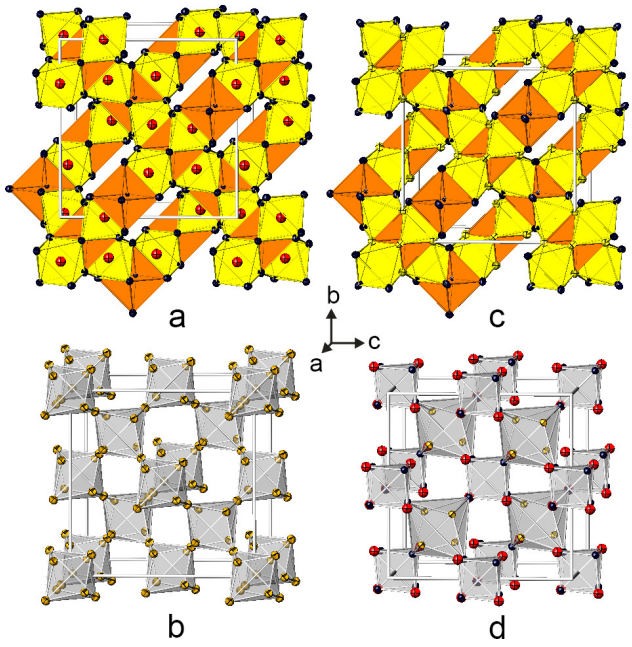

Fig. 3 Octahedral and tetrahedral frameworks in the structures Pd_3Cu_3B (a, b) and $Pd_5Cu_5B_2$ (c, d). Atom codes correspond to those given in Fig. 1.

Despite of sufficiently favorable spatial conditions, boron is not present in the [$Pd1_3Cu1_3$] octahedra, centered in the 16*e* site (*x*,*x*,*x*; *x*≈0.875, $d_{vac\text{-}Pd1}$≈0.2 nm, $d_{vac\text{-}Cu1}$≈1.94 nm) of $Pd_5Cu_5B_2$ structure; thus the octahedral network in the $Pd_5Cu_5B_2$ exhibits a linkage of four vertex-sharing empty octahedra (clustered around empty 4*c* (¼,¼,¼) and 4*b* (½,½,½) sites) (Fig. 3c) with slightly shorter edge lengths as compare to Pd_3Cu_3B ($d_{Pd1\text{-}Pd1}$=0.286 nm, $d_{Pd1\text{-}Cu1}$=0.281 nm, $d_{Cu1\text{-}Cu1}$=0.264 nm in $Pd_5Cu_5B_2$ *vs.* $d_{Pd1\text{-}Pd1}$=0.291 nm and $d_{Pd1\text{-}Pd1}$=0.308 nm in Pd_3Cu_3B). The tetrahedral framework in $Pd_5Cu_5B_2$ contains two distinct types of *tetrahedersterne* formed by different atoms ([$B1_4Pd2_4$] and [$Cu2_4Pd2_4$]) and is heavily distorted as compared to Pd_3Cu_3B ([$Cu1_4Cu2_4$], $d_{Cu1\text{-}Cu2}$=0.241 nm, $d_{Cu1\text{-}Cu1}$=0.264 nm) due to contrasting bond lengths ($d_{B1\text{-}Pd2}$=0.220 nm, $d_{Pd2\text{-}Pd2}$=0.284 nm and $d_{Cu2\text{-}Cu2}$=0.247 nm, $d_{Cu2\text{-}Pd2}$=0.272 nm in $Pd_5Cu_5B_2$ and Pd_3Cu_3B respectively) (Fig. 3d).

Electrical resistivity

Electrical resistivity of Pd_3Cu_3B, $Pd_5Cu_5B_2$ and $Pd_{5+x}Cu_{5-x}B_2$ (x=1) was studied using a 4-point method in a region from room temperature down to 0.3 K. From resistivity data the compounds behave metallically without any transitions in the entire temperature range (Fig. 4, Table 3). The resistivity curves for Pd_3Cu_3B and $Pd_5Cu_5B_2$ were analyzed in scope of the Bloch-Grüneisen relation,

$$\rho_{B-G} = \rho_0 + C\frac{T^5}{\theta_D{}^6}\int_0^{\theta_D/T}\frac{x^5}{(e^x-1)(1-e^{-x})}dx$$

revealing the Debye temperature $\theta_D = 221$ K and a residual resistivity $\rho_0 = 1.74\,\mu\Omega$cm for the first and $\theta_D = 229$ K and $\rho_0 = 20.2\,\mu\Omega$cm for the second compound, respectively. The former compound is also characterized by a high RRR ($RRR = \rho_{300}/\rho_0$) value of 9.8 pointing to a rather low degree of disorder in the sample.

The electrical resistivity of $Pd_{5+x}Cu_{5-x}B_2$ (x=1), in addition to its metallic behavior, demonstrates a noticeable curvature; as a consequence, an analysis with the simple Bloch-Grüneisen formula is not applicable anymore. Rather, a Mott-Jones term[56] (AT^3) has to be included to account for the corrections due to scattering of conduction electrons on a narrow band in the vicinity of the Fermi energy. Finally the least squares fit with

$$\rho = \rho_{B-G} + AT^3$$

delivered $\theta_D = 202$ K, $\rho_0 = 57.5\,\mu\Omega$cm and a Mott coefficient $A = -3.3*10^{-8}\,\mu\Omega$cm/K^3. The decreased value of RRR of ~1.2 points to increased disorder due to the presence of the (Pd,Cu) occupied sites, where Pd atoms destroy the "periodicity" of the lattice and thus increase the probability that an electron wave will be scattered.

Table 3 Residual resistivity ratio and least squares fit parameters, derived for the compound using the fit models described in text.

	ρ_0 [μΩcm]	θ_D [K]	A [μΩcm/K^3]	*RRR*
Pd_3Cu_3B	1.74	221	--	9.8
$Pd_5Cu_5B_2$	20.2	229	--	2.06
$Pd_{5+x}Cu_{5-x}B_2$ (x=1)	57.5	202	$-3.3*10^{-8}$	1.67

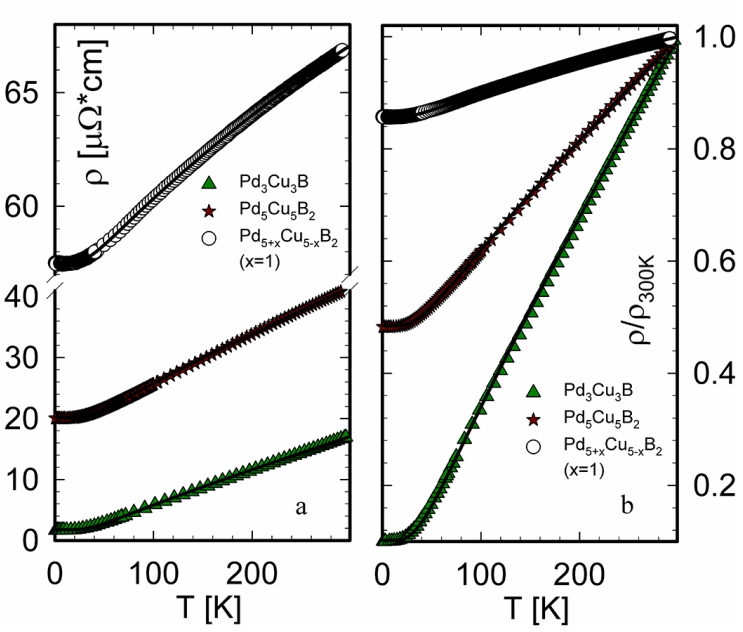

Fig. 4 The electrical resistivity of the compounds in PdCuB system (a). Same data represented as ρ / ρ_{300K} (b). Solid lines correspond to models described in text.

Electronic state

Total electronic density of states (DOS) of $Pd_5Cu_5B_2$ and Pd_3Cu_3B and their partial DOS for all atom sites are given in Fig. 5. For Pd_3Cu_3B, the *d*-states of Cu atoms supply the main contribution to the density of states below the Fermi level. The DOS spectra of Cu1 and Cu2 in

the presented energy range are similar; both of them differ from Pd1, which appears to have a rather diffuse distribution of *d*-states. In contrast to Pd_3Cu_3B, the partial density of states profiles of Pd1 and Pd2 in $Pd_5Cu_5B_2$ exhibit more localized and sharper distributions of *d*-states near -1 eV and -3 eV, suggesting that the contribution of Pd 4*d*- orbitals to the total density of states of this compound below the Fermi level is more prominent. Contribution of *d*-states of Pd1 (Pd_3Cu_3B) and Pd1 and Pd2 ($Pd_5Cu_5B_2$) to DOS above Fermi level is superior to those of Cu. At the Fermi level, the DOS also consist of Cu 3*d*- and Pd 4*d*-orbitals, and their partial charges are 7.79 (Pd1), 7.76 (Pd2), 9.23 (Cu1), and 9.24 (Cu2) for $Pd_5Cu_5B_2$, 7.77 (Pd), 9.16 (Cu1), and 9.17 (Cu2) for Pd_3Cu_3B. Below -5 eV, certain similarity is observed for the behavior of B 2*s*- and 2*p*- and Pd 4*d*-orbitals indicating their hybridization.

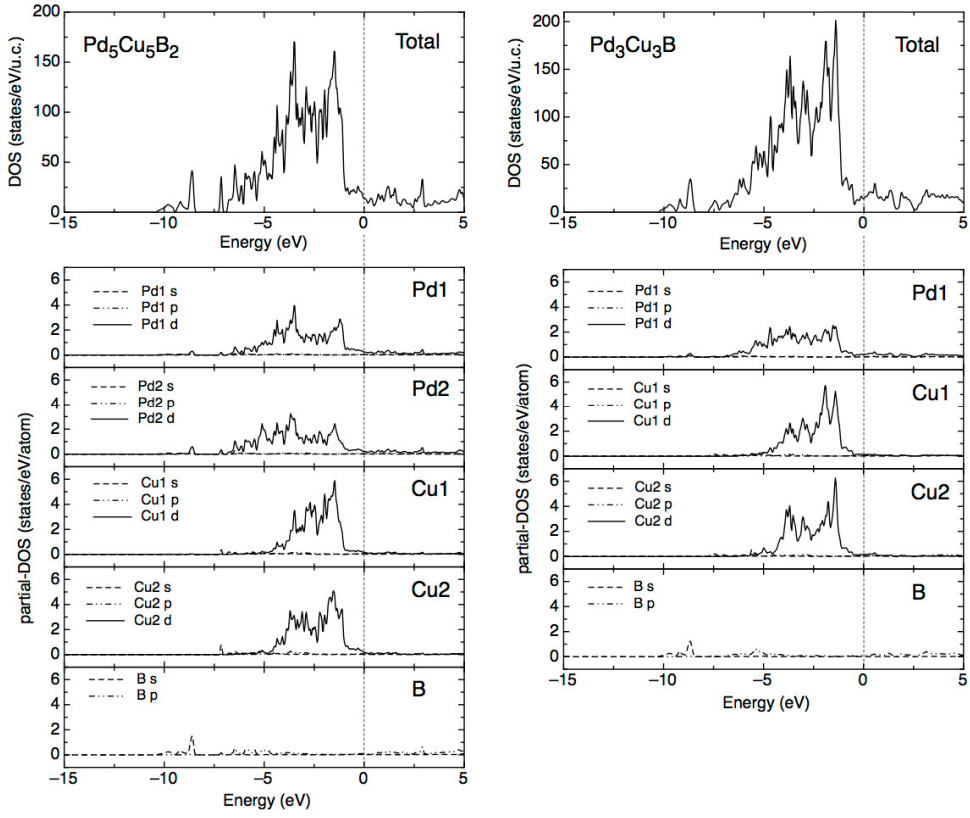

Fig. 5 Total electronic density of states of $Pd_5Cu_5B_2$ and Pd_3Cu_3B obtained from the electronic band structure calculation. Partial density of states of each atomic orbital for all atomic sites are also presented.

Formation of Pd_3Cu_3B and $Pd_5Cu_5B_2$ compounds

Historically, the investigations of compounds with Ti_2Ni-type derivative structures have been focused on iron carbides containing Mo and W due to formation of Fe_3Mo_3C and Fe_3W_3C (so called η-carbides), which were suggested to be responsible for the high strength, hardness, and toughness characteristics attributed to this class of tool steels. According to extensive studies, all hitherto reported variants of η-carbide structure crystallize with a centrosymmetric space group $Fd\bar{3}m$ and differentiate primarily by their stoichiometry (A:M:X) and atomic Wyckoff coordinates: unfilled Ti_2Ni-type (A:M:X=2:1:0), partially filled Ti_2Ni-type with ⅓ of the interstitial sites populated (A:M:X=6:6:1), partially filled Ti_2Ni-type with ⅔ of the interstitial sites populated (A:M:X=3:3:1 and A:M:X=4:2:1) and filled Ti_2Ni-type with all of the interstitial sites populated (A:M:X=4:2:1.5). Several carbide systems show the formation of two variants of η-carbide structure, for example the W-Fe-C[9,57] system where the W_6Fe_6C phase exhibits very small variations of lattice parameters indicating almost no homogeneity range (a=1.0956 nm to a=1.0958 nm) but the $(W_{3+x}Fe_{3-x})C$ compound forms with $0 \leq x \leq 1$ depending on the temperature as well as W-Co-C[9] and W-Ni-C[58] systems where the η-phases demonstrate a similar behaviour.

In A-M-C systems, the compositions of η-carbide phases are consistent with carbon atom occupancy of the interstitial octahedral sites. In contrast, in the Pd-Cu-B system the formation of an interstitial Ti_2Ni-type related structure is realized solely for the Pd_3Cu_3B composition. The manner in which Pd and Cu are accommodated in the metal atom framework of the Ti_2Ni-type structure is compatible with the distribution of atoms in the ordered derivatives of CdNi-type (Cd1 in 48*f*, Ni1 in 32*e* and Ni2 in 16*c*).[29] Notwithstanding metal η-carbides where the compositional range has been found to spread out between the A_3M_3C and A_4M_2C, Pd_3Cu_3B does not exhibit significant Pd/Cu compositional variability, according to EPMA data and evaluation of lattice parameters obtained from Rietveld refinement of X-ray powder diffraction data (a=1.11401(1) nm). The compound does not melt congruently and was observed from alloys annealed at 600 °C.

At slightly higher boron content (16.6 at. %), a boron atom occupies a metal site (namely one of the split Ti1 sites in noncentrosymmetric $F\bar{4}3m$ space group) thus producing a set of new compositions ($Pd_5Cu_5B_2$ - $Pd_{5+x}Cu_{5-x}B_2$ (x=1)) of the Ti_2Ni-type related structure. In as cast conditions, the composition range for $Pd_{5+x}Cu_{5-x}B_2$ varies due to a partial substitution of Cu atoms by Pd atoms on the 24*f* site and extends from 41.7 at.% Pd to about 50 at.% Pd

(a=1.053127(7) nm - 1.060640(5) nm) according to Pd/Cu ratios derived from EPMA. No substantial homogeneity range has been observed for the $Pd_5Cu_5B_2$ compound at 600 °C both from X-ray powder diffraction (a=1.052956(7) nm) and SEM data. Akin η12- and η6-carbides (e.g. Mo_6Co_6C and Mo_3Co_3C[8]), the Pd_3Cu_3B and $Pd_5Cu_5B_2$ phases show no mutual solid solubility in alloys annealed at 600 °C.

Conclusions

The Pd-Cu-B system represents an unique example of the formation of both inclusion and substitutive derivatives of the Ti_2Ni-type structure, the Pd_3Cu_3B and $Pd_5Cu_5B_2$ structures, respectively. While both compounds exist in alloys annealed at 600 °C, the only boron rich phase forms directly from the melt and exhibits in as cast conditions an extended homogeneity field stretching up to almost 50 at.% Pd as derived from X-ray powder diffraction data supported by SEM analysis. No perceptible homogeneity range was observed for Pd_3Cu_3B. Two phases in annealed conditions exist as distinct compounds exhibiting no mutual solid solubility.

Pd_3Cu_3B (space group $Fd\bar{3}m$) is a boron-poor Ti_2Ni-type derivative structure and obeys the interstitial principle of formation, recognizable from the parallelism to the corresponding ternary metal carbide W_3Fe_3C. Consequently, B is located in octahedral 16*d* site ($[BPd_6]$) while metal atoms distribution corresponds to the accommodation of atoms in the CdNi-type structure with Pd occupying the Cd position and Cu populating the Ni site. $Pd_5Cu_5B_2$, a boron-rich Ti_2Ni-type derivative structure, exhibits a non-centrosymmetric substitutive boride type of η-carbides. Boron is found in ($[BPd_6]$) trigonal prisms. The reduction of symmetry on passing from the Ti_2Ni-type structure to $Pd_5Cu_5B_2$ corresponds to the loss of the $\bar{3}$ axis delivered by the ordered occupation of the Ni position (32*e*) by dissimilar atoms, Cu and B. Reorganization of atoms in the unit cell on increasing the boron content (Pd in 48*f* is replaced by Pd and Cu both located in 24*g*; Cu in 32*e* is substituted by Cu and B in 16*e*; Pd in 16*e* takes the place of Cu in former 16*c* position) leads to a substantial decrease of the $Pd_5Cu_5B_2$ lattice parameter (a=1.05273(5) nm) as compared to Pd_3Cu_3B (a=1.1135(3) nm).

As in few other copper transition metal borides known so far,[40,58-60 59-61 - to correct in proofs] copper atoms are not found in the first coordination sphere of boron atoms. The Pd_3Cu_3B structure exhibits two interpenetrating frameworks of which one is composed of $[Cu_6]$ empty

super-tetrahedra while another one is formed by [BPd_6] octahedra. While the absence of boron in the [Pd_3Cu_3] octahedral voids leads merely to a slight condensation of octahedra in the octahedral framework in the $Pd_5Cu_5B_2$ structure, the boron participation in the metal atom network delivers a heavy distortion of the tetrahedral framework of $Pd_5Cu_5B_2$ as compared to Pd_3Cu_3B.

In the light of the nested polyhedra model description, the $Pd_5Cu_5B_2$ structure is geometrically composed of γ-brass type nested units and groups of tetrahedrally oriented borons which are bonded with the Pd atoms of the octahedral shell of the γ-brass cluster. Similarly, the γ-brass type nested polyhedra are present in the Pd_3Cu_3B structure, however the spacers are formed by two tetrahedrally oriented groups of atoms, namely four Cu and four B.

The temperature dependant electrical resistivity and electronic states calculations of compounds investigated demonstrate metallic behavior. The influence of the *s-d* electron scattering mechanism on the resistivity is negligible for $Pd_5Cu_5B_2$ but becomes pronounced for $Pd_{5+x}Cu_{5-x}B_2$.

Acknowledgements

The research work of O.S. was supported by Austrian FWF project V279-N19. Authors are very thankful to Dr. Klaudia Hradil (XRC TU Wien) for collaboration and to Mrs. Monika Waas for SEM measurements.

Supporting information

Supplementary data associated with this article (Rietveld X-ray powder diffraction refinements of Pd_3Cu_3B, $Pd_5Cu_5B_2$ and $Pd_{5+x}Cu_{5-x}B_2$) can be found in the online version at ….

Notes and references

1 G. A. Yurko, J. W. Barton and J. G. Parr, Acta Cryst., 1959, 12, 909-911.

2 A. Westgren, Jernkontorets Ann., 1933, 17, 1-14.

3 K. Kuo, Acta Metall., 1953, 1, 301-304.

4 W. Jeitschko, H. Holleck, H. Nowotny and F. Benesovsky, Monatsh. Chem., 1964, 95, 1004-1006.

5 W. Jeitschko, H. Nowotny and F. Benesovsky, Monatsh. Chem., 1964, 95, 156.

6 H. Nowotny, W. Jeitschko and F. Benesovslky, Planseeber. Pulvermetallurgie, 1964, 12, 31.

7 H. Nowotny, Prog. Solid State Chem., 1971, 5, 27–70.

8 J. M. Newsam, A. J. Jacobson, L. E. McCandlish and R.S. Polizzotti, J. Solid State Chem., 1988, 75, 296-304.

9 C. B. Pollock and H. H. Stadelmaier, Metallurg. Trans., 1970, 1, 767-770.

10 S. Sridharan, H. Nowotny and S. F. Wayne, Monatsh. Chem., 1983, 114, 127-135.

11 J. Etzkorn and H. Hillebrecht, J. Solid State Chem., 2008, 181, 1342–1346.

12 S. M. Hunter, D. H. Gregory, J. S. J. Hargreaves, M. Richard, D. Duprez and N. Bion, ACS Catal., 2013, 3, 1719−1725.

13 S. M. Hunter, D. Mckay, R. I. Smith, J. S. J. Hargreaves and D. H. Gregory, Chem. Mater., 2010, 22, 2898–2907.

14 S.K. Jackson, R.C. Layland and H.-C. zur Loye, J. Alloys Comp., 1999, 291, 94-101 and the references herein.

15 T. J. Prior and P. D. Battle, J. Mater. Chem., 2004, 14, 3001-3007.

16 N. Karlsson, Nature, 1951, 168, 558.

17 M. Kotyk and H. H. Stadelmaier, Metallurg. Trans., 1970, 1(4), 899-903.

18 M. Polak, M. Hefetz, M. H. Mintz and M. P. Dariel, J. Electron Spectrosc. Relat. Phenom., 1983, 31(3), 199–206.

19 B. Rupp and P. Fischer, J. Less-Comm. Met., 1988, 144(2), 275–281.

20 R. Mackay, G. J. Miller and H. F. Franzen, J. Alloys. Comp. 1994, 204(1–2), 109–118.

21 P. Rogl and H. Nowotny, Monatsh. Chem. 1977, 108, 1167-1180.

22 B. Huneau, J. J. Ding, P. Rogl, J. Bauer, X. Y. Ding and M. Bohn, J. Solid State Chem. 2000, 155, 71-77

23 E. L. Kugler, L. E. McCandlish, A. J. Jacobson and R. R. Chianelli, United States Patent, 1992, 5, 138, 111.

24 H. Buchner, M. A. Gutjahr, K. D. Beccu and H. Säufferer, Z. Metallkd., 1972, 63, 497-500.

25 Hydrogen as a Future Energy Carrier, Ed. A. Züttel, A. Borgschulte and L. Schlapbach, WILEY-VCH Verlag GmbH and Co. KGaA, 2008 and the references herein.

26 D. G. Westlake, J. Chem. Phys., 1983, 79, 4532-4538..

27 F. J. Rotella, H. E. Flotow, D. M. Gruen and J. D. Jorgensen, J. Chem. Phys., 1983, 79, 4522-4531.

28 A. M. Alekseeva, A. M. Abakumov, A. Leithe-Jasper, W. Schnelle, Yu. Prots, P. S. Chizhov, G. Van Tendeloo, E. V. Antipov and Yu. Grin, J. Solid State Chem., 2006, 179 2751–2760.

29 J. K. Critchley and J. W. Jeffery, Acta Crystallogr., 1965, 19, 674-676.

30 P. P. Jana and S. Lidin, Cryst. Eng. Comm., 2013,15, 745-75.

31 G. J. Snyder and A. Simon, J. Chem. Soc. Dalton Trans., 1994, 7, 1159-1160.

32 P. Villars and K. Cenzual, Pearson's Crystal Data: Crystal Structure Database for Inorganic Compounds, ASM International®, Materials Park, Ohio, USA.

33 E. I. Gladyshevskii, Yu. B. Kuz'ma and I. Kripyakevich, J. Struct. Chem., 1963, 4, 343-349.

34 K. J. Range, F. Rau and U. Klement, Acta Cryst., 1990, C46, 2454-2455.

35 N. F. Chaban and Y. B. Kuz'ma, Inorg. Mater., 1972, 8, 933-936.

36 U. Ch. Rodewald, S. Tuncela, B. Chevalier and R. Pöttgen, Z. Anorg. Allg. Chem., 2008, 634, 1011-1016 and the references herein.

37 P. Solokha, S. De Negri, V. Pavlyuk and A. Saccone, Chem. Met. Alloys, 2009, 2, 39-48.

38 R. Noebe, T. Biles and S.A. Padula, NiTi-Based High-Temperature Shape-Memory Alloys: Properties, Prospects, and Potential Applications in Advance structural materials: properties, design optimization, and applications Ed. W. Soboyejo (2006) CRC Press, Taylor & Francis Group, 145-186.

39 Saif ur Rehman, M. Khan, A. N. Khan, S. H. I. Jaffery, L. Ali and A. Mubashar, Adv. Mat. Science and Engin., 2015, 434923, 7 pages.

40 L. P. Salamakha, O. Sologub, B. Stöger, H. Michor, E. Bauer and P.F. Rogl, J. Solid State Chem. 2015, 229, 303-309.

41 J. Rodriguez-Carvajal, Physica B, 1993, 192, 55-69.

42 P. Blaha, K. Schwarz, G. K. H. Madsen, D. Kvasnicka and J. Luiz, WIEN2K, University of Technology, Vienna, 2001.

43 Bruker. Advanced X-ray solutions. APEX2 User Manual. Version 1.22. 2004, Bruker AXS Inc.

44 Bruker. APEXII, SAINT and SADABS. 2008, Bruker Analytical X-ray Instruments, Inc., Madison, Wisconsin, USA.

45 G. M. Sheldrick, SHELXS-97, Program for the Solution of Crystal Structures; University of Göttingen, Germany, 1997.

46 G. M. Sheldrick, SHELXL-97, Program for Crystal Structure Refinement; University of Göttingen, 1997.

47 L. J. J. Farrugia, Appl. Cryst., 1999, 32, 837-838.

48 E. Parthé, L. Gelato, B. Chabot, M. Penzo, K. Censual and R. Gladyshevskii, TYPIX – Standardized Data and Crystal Chemical Characterization of Inorganic Structure Types; Berlin: Springer, 1994.

49 B. Chabot, K. Cenzual and E. Parthé, Acta Cryst., 1981, A37, 6-11.

50 A. J. Bradley and P. Jones, J. Inst. Met. 1933, 51, 131.

51 S. Thimmaiah and G. J. Miller, Chem. Eur. J., 2010, 16(18), 5461–5471.

52 O. Gourdon, D. Gout, D.J. Williams, T. Proffen, S. Hobbs and G.J. Miller, Inorg. Chem., 2007, 46, 251-260.

53 A. A. Pankova, V. A. Blatov, G. D. Ilyushin and D. M. M. Proserpio, Inorg. Chem., 2013, 52, 13094−13107.

54 E. A. Lord and S. J. Ranganathan, J. Non-Cryst. Solids, 2004, 334−335, 121-125.

55 E. A. Lord, A. L. Mackay and S. Ranganathan, New Geometries for New Materials; Cambridge University Press: Cambridge, U.K., 2006.

56 O. Gunnarsson, M. Calandra and J. E. Han, Rev. Mod. Phys. 2003, 75, 1085.

57 D. C. Azubike, A. Chrysanthou and U. O. Igiehon, Powder Diffr., 1992, 7, 162-163.

58 P. Ettmayer and R. Suchentrunk, Monatsh. Chem. 1970, 101(4), 1098-1103.

59 W. Klünter, B. Schmidt and W. Jung, J. Alloys Compd., 1994, 205, 93-100

60 W. Klünter and W. Jung, Z. Anorg. Allg. Chem., 2000, 626, 502-505.

61 O. Sologub, L. P. Salamakha, P. F. Rogl, B. Stöger, E. Bauer, J. Bernardi, G. Giester, M. Waas and R. Svagera, Inorg. Chem, 2015, 54 (22), 10958–10965.

TOC

Arrangements of B structural units in the new Ti_2Ni-type derivative boride structures.